Since January 2020 Elsevier has created a COVID-19 resource centre with free information in English and Mandarin on the novel coronavirus COVID-19. The COVID-19 resource centre is hosted on Elsevier Connect, the company's public news and information website.

European Journal of Radiology 136 (2021) 109548

Contents lists available at ScienceDirect

European Journal of Radiology

journal homepage: www.elsevier.com/locate/ejrad

Review

Radiological, epidemiological and clinical patterns of pulmonary viral infections

Konstantinos Stefanidis [a,*], Elissavet Konstantelou [b], Gibran Timothy Yusuf [a], Anastasia Oikonomou [c], Kyriaki Tavernaraki [d], Dimitrios Karakitsos [e], Stylianos Loukides [f], Ioannis Vlahos [g]

[a] Radiology Department, King's College Hospital NHS Foundation Trust, London, UK
[b] 1st Respiratory Department of the National and Kapodistrian University of Athens, "Sotiria" General and Chest Diseases' Hospital, Athens, Greece
[c] Department of Medical Imaging, Sunnybrook Health Sciences Centre, University of Toronto, Canada
[d] Imaging and Interventional Radiology, Sotiria General and Chest Diseases Hospital, Athens, Greece
[e] Critical Care Department, King Saud Medical City, Riyadh, Saudi Arabia
[f] 2nd Respiratory Department of the National and Kapodistrian University of Athens, "Attikon" General Hospital, Athens, Greece
[g] Department of Thoracic Radiology, Division of Diagnostic Imaging. University of Texas MD Anderson Cancer Center, Houston, TX, USA

ARTICLE INFO

Keywords:
Respiratory viruses
Imaging
Computed Tomography
Chest x-ray
Clinical presentation
Epidemiology
Diagnosis
Differential diagnosis

ABSTRACT

Respiratory viruses are the most common causes of acute respiratory infections. However, identification of the underlying viral pathogen may not always be easy. Clinical presentations of respiratory viral infections usually overlap and may mimic those of diseases caused by bacteria. However, certain imaging morphologic patterns may suggest a particular viral pathogen as the cause of the infection. Although definitive diagnosis cannot be made on the basis of clinical or imaging features alone, the use of a combination of clinical and radiographic findings can substantially improve the accuracy of diagnosis. The purpose of this review is to present the clinical, epidemiological and radiological patterns of lower respiratory tract viral pathogens providing a comprehensive approach for their diagnosis and identification in hospitals and community outbreaks.

1. Introduction

The emergence of the novel Coronavirus disease in December 2019 (Covid-19) in Wuhan (Hubei, China), caused by SARS-CoV-2 (Severe Acute Respiratory Syndrome Coronavirus 2) and the ongoing pandemic as a result of the viral spread, have once more drawn physicians' attention to respiratory viruses and have re-emphasized the role of viral pathogens as cause of severe pneumonia. Throughout human history, outbreaks of respiratory diseases due to viruses have commonly been reported. Epidemics of smallpox in the Roman Empire and Japan during the first century AD are among the first known outbreaks of viral diseases [1,2]. Since then, multiple epidemics caused by other viruses have been recorded. Influenza type A virus pandemic (H1N1 subtype), known as the "Spanish flu", was the most devastating leading to approximately 100,000,000 deaths worldwide from 1918 to 1920 [3]. During the 21 st century new viral outbreaks were reported: SARS that surfaced in 2002, caused by the SARS coronavirus strain 1 (SARS-CoV-1), resulted in hundreds of deaths, mostly in China and Hong Kong. Since 2003 sporadic cases of H5N1 influenza (Asian Avian Influenza A) have occurred, whereas in 2009–2010 and in 2015 H1N1 flu pandemics ("Swine flu") resulted in thousands of fatal cases worldwide [3]. In 2012 another coronavirus strain ("Middle East respiratory syndrome – MERS coronavirus") emerged and has been responsible for some hundreds of deaths so far [3–5].

The fatal burden of viral outbreaks throughout human history, as well as the fact that new respiratory viruses have been discovered during the past decade, highlight the pathogenic role of viruses in respiratory disease, including community acquired pneumonia (CAP). Diagnosis of viral pneumonia depends on clinical criteria, epidemiological factors (e.g. presence of viral epidemics in the community and seasonality of viral pathogens) and laboratory findings, including molecular detection techniques [6]. However, imaging plays a significant role in patient management, as it is necessary for determining the severity and extension of the infection. Accurate and early diagnosis of the various viral

* Corresponding author.
E-mail address: kstefanidis@nhs.net (K. Stefanidis).

https://doi.org/10.1016/j.ejrad.2021.109548
Received 21 November 2020; Received in revised form 8 January 2021; Accepted 11 January 2021
Available online 14 January 2021

Table 1
Seasonal variation of respiratory tract viral infection pathogens in the Northern hemisphere. Seasonal patterns and peak incidence of the various viral pathogens are different in the Southern hemisphere depending on season and latitude. INF, influenza; RSV, respiratory syncytial virus; PIV, parainfluenza; hMPV, Metapneumovirus.

JAN	FEB	MAR	APR	MAY	JUN	JUL	AUG	SEP	OCT	NOV	DEC
	INF									**INF**	
					RHINOVIRUS						
	CORONAVIRUS										
		RSV								**RSV**	
						PIF					
						ADENOVIRUS					
		hMPV									

pathogens through a multimodality approach is crucial, as specific therapies are available against certain viruses. In this article, we review concurrently the epidemiological, clinical and radiological features of pathogens causing viral pneumonia.

2. Epidemiology

It is estimated that viruses are responsible for 15%–56% of CAP in hospitalized immunocompetent patients, either by themselves or as co-pathogens with bacteria [7–10]. The variability of the reported proportion of viral pneumonias from various studies may be explained by differences in study populations and the testing rigor for viruses. Moreover, even when viral testing is undertaken, the true incidence of viral pneumonias remains unclear and probably underestimated as upper respiratory sampling (nasal swab, nasopharyngeal swab) is most commonly performed compared to the most sensitive but less easy lower respiratory sampling [bronchoalveolar lavage (BAL) fluid, tracheal aspirates, induced sputum], [7–10]. Regardless of viral testing accuracy, immunocompromised patients, especially those who have undergone hematopoietic stem cell or solid organ transplantation or patients under chemotherapy for leukaemia, demonstrate a significantly higher incidence of viral pneumonias [11]. In this population viral pneumonias are typically more severe and associated with higher mortality rates, compared to healthy subjects [11]. Additionally, it has been shown that the incidence of lower respiratory infections is higher in the very young and the elderly [12]. Consequently, in order to narrow the differential diagnosis of the various pathogens in a case of pneumonia, it is important not only to consider patient characteristics (immune state, age, co-morbidities), but also a patient's travel and epidemiological factors (e.g. seasonality of viral infections, current epidemics).

3. Seasonality

Seasonality is one of the defining characteristics of viral respiratory infections, although the aetiology for this observation is not fully elucidated [13,14]. Various epidemiological studies have shown that the frequency of respiratory infections increases rapidly in the autumn, remains high throughout the winter and decreases in the spring in temperate regions of the northern hemisphere (Table 1) [13,14]. A combination of factors seems to be responsible for the seasonality of viral infections: increased viral survival due to low environmental humidity and temperature during winter, diminished daylight and vitamin D deficiency resulting in wintertime relative immunosuppression, rapid spreading of the viruses because of increased people crowding and school opening during autumn and winter [15–19]. In tropical areas, most viral infections arise during the rainy season [20].

4. Clinical features

The clinical presentation of viral pneumonias is variable, depending on the causative organism and the immune status and comorbidities of the host (Table 2). Viral pneumonias present in a much more severe form in immunocompromised patients, the elderly or those of very young age [12]. Institutionalization and cardiac co-morbidities seem to be additional risk factors [8].

Viral pneumonias in general have similar clinical symptoms (cough, shortness of breath, increased sputum, chest pain) and signs (fever, tachycardia, tachypnoea, hypoxia) with bacterial pneumonias [6]. However, some clinical features are noted more often in viral infections, such as cough and myalgia [7,21]. Features such as rhinitis, conjunctivitis and pharyngitis are also usual clinical manifestations of viral pneumonias. Moreover, as compared to bacterial pneumonia, in viral pneumonitis leucocytosis is less frequently seen and procalcitonin levels are lower [6].

It is clinically recognized that radiological findings may contribute to the differentiation of viral from bacterial pneumonias. Ruuskanen et al. have proposed a set of combined clinical, radiological, epidemiological and laboratory criteria that may predict viral aetiology of pneumonia in patients [6]. Nonetheless, predicting the viral aetiology from clinical, laboratory or radiological parameters remains imprecise. In the absence of isolation of a viral pathogen, there is no clinico-radiological gold standard for differentiating the aetiology of pneumonia [22].

Differential diagnosis is rendered even more challenging by the fact that viral pneumonias are often complicated by bacterial superinfections, which are typically associated with worsening of the prognosis. For example, influenza pneumonia is frequently associated with Streptococcus Pneumoniae, Haemophilus Influenzae and Staphylococcus Aureus (including Methicillin-resistant S. Aureus) co-infection, whereas rhinovirus pneumonia is associated with Streptococcus pneumonia co-infection [23,24]. Specifically, during the 2009 H1N1 pandemic, 4%–24 % of cases presented with bacterial co-infection [25–27].

Therefore, in summary, secondary bacterial infection must be considered in every case of probable viral pneumonia and should be treated presumptively until full identification of the pathogens involved is obtained.

5. Laboratory identification methods

The detection of virus or specific viral antigens in respiratory tract samples has traditionally been done by culture and immunofluorescence microscopy. Additionally, antibody seroconversion during the clinical course of the disease, has also been performed for years [28]. Improvements in molecular detection techniques, particularly real time techniques such as reverse transcription polymerase chain reaction (RT-PCR), have enabled assessment of the proportion of CAP caused by specific organisms, and viruses as a whole. In particular, the advent of fast and reliable viral genome sequencing using PCR has facilitated the detection of many viral causes of pneumonia, some of which were previously unknown such as human metapneumovirus [29]. PCR techniques are reported to be 2–5 times more sensitive than conventional methods for the detection of respiratory viruses [30].

Clinical specimens that are suitable for diagnosis of viral pneumonia include, in order of preference: lung tissue and BAL fluid, nasopharyngeal wash samples, nasopharyngeal swabs and sputum. Lung tissue and BAL are often unavailable because of their invasive nature, but nevertheless are very useful in immunocompromised and critically ill patients, in whom a specific diagnosis is necessary and co-infections are

Table 2
Clinical characteristics of the viral infections of the respiratory tract. PIV, parainfluenza; RSV, respiratory syncytial virus; hMPV, human metapneumovirus, HSV, herpes simplex virus; VSV, varicella-zoster virus; CMV, cytomegalovirus.

	Viral Pathogen	Signs and Symptoms	Risk factors -populations at risk	Transmission	Incubation
RNA virus	**Influenza**	From mild flu-like symptoms to severe pneumonia	Immunosuppression, obesity, elderly, pregnancy	Highly contagious via contact with respiratory secretions or inhalation of droplets or aerosols	18–72 hours
	PIV	Upper tract respiratory infections, bronchitis, pneumonia in children, mild symptoms in adults	COPD, asthma, Closed populations (nurseries, day care centers)	Respiratory secretions or inhalation of droplets or aerosols	3–6 days
	RSV	Upper respiratory tract infections (coryza, pharyngitis), Flu-like illness, Bronchiolitis Pneumonia Asthma-COPD exacerbation	Cardiopulmonary disease, immunosuppression, Hematologic malignancies, bone marrow transplantation, infants and children	Respiratory secretions or inhalation of droplets or aerosols	4–6 days
	Rhinovirus	Mild cold symptoms, bronchitis, bronchiolitis, pneumonia, asthma – COPD exacerbation	COPD, asthma, cystic fibrosis, infants and children	Respiratory secretions or inhalation of droplets or aerosols	1–3 days
	hMPV	Common cold, bronchiolitis, pneumonia	Immunosuppression, elderly, cardiopulmonary disease	Respiratory secretions or inhalation of droplets or aerosols	4–6 days
	SARS-MERS	Common cold to severe pneumonia-ARDS	Immunosuppression, elderly, cardiopulmonary disease	Respiratory secretions or inhalation of droplets or aerosols	2–7 days
	Covid-19	Common cold to severe pneumonia-ARDS, anosmia-GI symptoms	Immunosuppression, elderly, cardiopulmonary disease	Highly contagious via contact with respiratory secretions or inhalation of droplets or aerosols	5–6 days
DNA virus	**Adenovirus**	Similar to influenza with abrupt onset of fever	Immunosuppression, organ/Bone marrow transplantation, closed population (military facilities, hospital wards)	Respiratory secretions or inhalation of droplets or aerosols	4–7 days
	HSV	Dyspnea, cough, fever, tachypnea, chest pain, hemoptysis, pneumonia, ARDS	Immunosuppression, burns, malignancy, organ transplantation	Contact with contaminated respiratory secretions – mucus membranes or herpetic ulcers, hematogenous dissemination from mucocutaneous lesions	1 week
	VZV	Fever, rash, fluid-filled blisters, pneumonia	Immunosuppression, hematologic malignancies, immunodeficiency, children	Highly contagious via contact with aerosols, particles, droplets or blisters from infected patient	2 weeks
	CMV	Prolonged fever, lack of cough, variable clinical manifestation in immunosuppressed	Immunosuppression, bone marrow transplant, HIV	Direct contact, sexual intercourse, birth canal passage, breast milk ingestion, transfusion and organ/bone marrow transplantation	28–60 days
	Hantavirus	Common cold to severe pneumonia-ARDS	Pest control workers, exposure to rodents	Via inhalation of aerosolised virus-contaminated rodent excreta	1–2 weeks

common [31].

6. Chest x-ray and CT patterns

Improvements in imaging technology, in particular the availability of high-resolution CT, coupled with the growing number of detectable pathogenic organisms in atypical pneumonia, provide both opportunities and challenges for the radiologist.

Chest x-ray is the first screening tool for the detection of an active infective process. However, it has been shown that it is of limited value predicting aetiology of lower respiratory tract infection as it is frequently non-specific, demonstrating normal or subtle findings [32]. CT imaging provides further detailed information with different patterns (Table 3). However, the significant overlap of imaging features between pathogens limits the identification of specific causative organisms. Specifically, co-infection with multiple viral and bacterial pathogens, estimated in several studies to occur in around 15 % of the cases, can further complicate diagnosis [7,33].

7. Selected RNA viruses

7.1. *Influenza virus*

Influenza virus belongs to the orthomyxovirus family of RNA viruses. There are three groups of influenza viruses (A, B and C) of which type A virus is the most virulent and can easily mutate [34]. In temperate climates, epidemics are seen almost exclusively in the winter months (generally November to April in the Northern hemisphere and May to September in the Southern hemisphere), whereas in tropical areas, influenza infection is reported throughout the year [13,14]. Influenza can cause a spectrum of clinical disease ranging from relatively mild upper respiratory tract infection with flu-like symptoms, to fulminant and overwhelming pneumonia which occurs particularly in the elderly and immunocompromised.

Histopathologic studies have showed that severe influenza is characterized by necrotizing bronchitis, capillary and small-vessel thrombosis, interstitial oedema and inflammatory infiltrates, the formation of hyaline membranes, haemorrhage, as well as diffuse alveolar damage (DAD) [35].

Paralleling the histopathological picture, there is a broad range of reported imaging appearances in influenza pneumonia. Findings at initial chest x-ray in patients with H1N1 influenza include central or peripheral ground glass opacities and consolidation with a patchy or nodular appearance [36] (Figs. 1, 2). Aviram et al. have showed that the initial chest radiographic findings have also a prognostic role predicting clinical outcome. Specifically, there is association of multizonal and bilateral peripheral opacities with progression to respiratory failure requiring mechanical ventilation and poor clinical outcome [36].

A normal CT scan is seen in approximately half of patients with proven influenza virus disease [37]. In those with abnormal findings, ground glass opacities, multifocal consolidation or a combination of ground glass opacity and consolidation is the commonest pattern. A predominant peribronchovascular and subpleural distribution, has been described, resembling organizing pneumonia [37]. Interlobular septal thickening and centrilobular nodules are also common findings [38–40]. Bilateral patchy consolidation, ill-defined small nodules, and patchy ground glass opacities associated with the areas of consolidation have been reported in patients with underlying hematologic malignancy [41].

7.2. *Parainfluenza virus*

The human parainfluenza virus (PIV) belongs to the Paramyxoviridae family and is separated into 4 types accounting for 2–4 % of CAP cases in adults [42,43]. Type 3 is the most common form and related to acute illness in immunocompromised patients [44,45]. Epidemiological data demonstrate distinct seasonality for all four types

Table 3
Summary of CT findings in viral lower respiratory tract infections. The relative frequency of the CT findings are indicated with plus (+) signs from lowest (+) to the highest (+++). RSV, respiratory syncytial virus; hMPV, human metapneumovirus; CMV, cytomegalovirus.

Viral pathogen	Centrilobular nodules, micronodules, tree-in-bud	Ground-glass opacification	Consolidation	Reticularinterstitial
Influenza	+++	+++	+	+
Parainfluenza	+++	+++	+	+
RSV	+++	+++	+	–
Rhinovirus	++	++	+	+
hMPV	+++	+++	++	+
Coronavirus	–	+++	++	++
Adenovirus	–	++	+	++
CMV	++	++	++	–
Varicella-zoster	+++	+	+	–

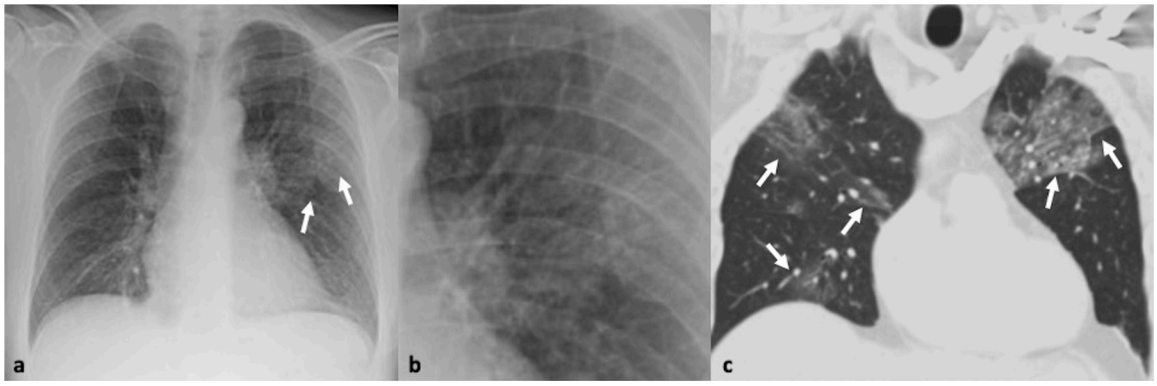

Fig. 1. 41-year-old male with confirmed influenza pneumonia who presented with fever, dry cough and myalgia. 1a, b. Chest x-ray and magnified view shows left upper lobe patchy increased air-space opacification (arrows). 1c. Coronal CT image confirms the left upper lobe ground glass opacity and further multifocal ground glass involvement in both lungs (arrows).

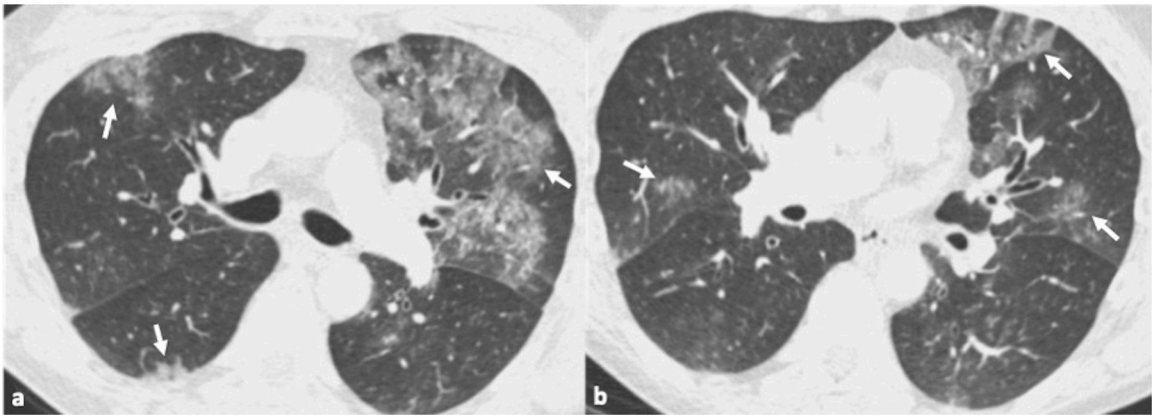

Fig. 2. 45-year-old male patient with confirmed influenza pneumonia. 2a, b. Axial CT images show multifocal patchy ground glass opacities (arrows).

with type 3 more prevalent in the spring and summer [13,14]. PIV can cause upper tract respiratory infections (rhinitis, pharyngitis, laryngitis), as well as more severe manifestations such as bronchiolitis and pneumonia. Infections are usually associated with histological patterns of bronchiolitis and DAD.

The radiographic appearance of PIV infections is not specific and includes opacities and nodules. The virus presents with a predominantly airway-centric pattern of disease on CT [46]. Findings include ground glass opacities, consolidation, tree-in-bud nodules and bronchial wall thickening [34,44–46] (Fig. 3). PIV infections appear to affect the lower lobes more which may assist differentiation from other viral infections such as influenza and RSV [34].

7.3. Respiratory syncytial virus

Respiratory syncytial virus (RSV) is classified in the Pneumovirus genus of the Paramyxoviridae family. Although RSV is the most frequent viral pathogen causing lower respiratory tract infection in infants, it is now recognized as a significant pathogen especially in immunocompromised adults particularly with a haematological or autoimmune primary disease [47–49]. Similar to the influenza viruses, RSV causes outbreaks of respiratory illness in the late fall, winter or spring [13,14]. In infants and children, RSV infection is usually associated with upper respiratory tract illness manifestations. In immunosuppressed adults, RSV infection manifests with severe lower respiratory tract complications which can result in serious morbidity and significant mortality. Whimbey and Ghosh evaluated the role of community respiratory viral infections in hospitalized adult bone marrow transplant recipients and

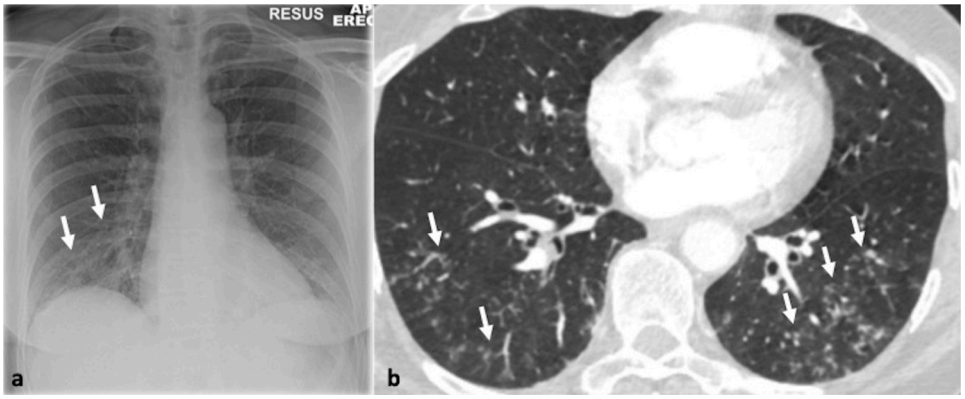

Fig. 3. 54-year-old woman with fever and cough. Parainfluenza was the only pathogen recovered from respiratory secretions. 3a. Chest x-ray shows reticulonodular opacities in the right lower zone (arrows). 3b. Transverse thin section CT scan confirms the presence of multiple micronodules and branching opacities (arrows).

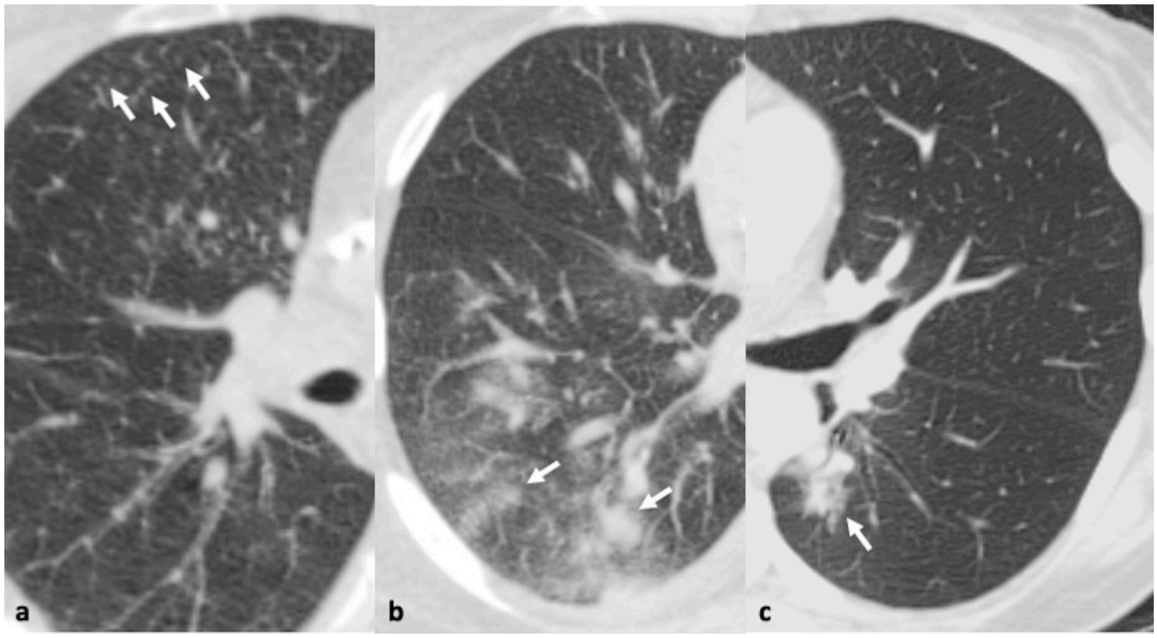

Fig. 4. 51-year-old woman with confirmed respiratory syncytial virus infection. 4a-c. Transverse thin section CT scan through the mid and lower zones demonstrates a few tiny nodules (arrows, a) and bilateral patchy areas of nodular ground glass opacity and consolidation (arrows b, c).

found an incidence of RSV pneumonia of 9.2 % with a mortality rate of 60 % [50].

The histopathology of RSV bronchiolitis is most commonly described as plugging or occlusion of bronchiolar airway lumens by sloughed necrotic and irregular epithelium, combined with peribronchiolar infiltration and submucosal oedema [51].

In children, chest x-ray may be normal or abnormal with features of central airspace opacification and peribronchial thickening [52,53]. In adults and elderly patients, chest x-ray generally does not distinguish RSV pneumonia from bacterial infection and most commonly demonstrate bilateral alveolar opacities but may also show interstitial changes [54]. On CT, RSV pneumonia typically shows an airway-centric pattern of disease, with ground glass opacities, nodules, small focal areas of consolidation and bronchial wall thickening [47,48,55] (Fig. 4). Especially during the early phase, the CT findings may be more characteristic with nodules and tree-in-bud opacities [55]. When nodules are present, a peripheral halo of ground-glass is common (70 %) and may assist in narrowing the differential diagnosis [55].

7.4. Rhinovirus

Rhinovirus (RV) is encountered in the RNA Enterovirus genus in the Picornaviridae. RV is a major pathogen of respiratory infection detected in 18 %–26 % of paediatric patients and in 2%–17 % of adult patients with CAP [56,57]. RVs infections are reported to be more prevalent in the early fall and late spring [13,14,58]. It can cause a wide spectrum of upper and lower respiratory tract manifestations, varying from mild episodes of coryza, scratchy throat, rhinorrhoea, pharyngitis and bronchitis to pneumonia or bronchiolitis frequently associated with exacerbation of asthma and chronic obstructive pulmonary disease [59,60].

The histological findings mirror the radiological appearances. RV by itself does not destroy the airway epithelial barrier with no cytopathic effect on the respiratory epithelium. However, it can cause disruption of the epithelial barrier, which leads to increased vascular permeability and mucous secretion [61]. Therefore, while normal or almost normal appearances can be found in mild disease, in patients with severe rhinovirus pneumonia, a peribronchial and interstitial pattern with ground glass opacity is most commonly noted [62] (Fig. 5).

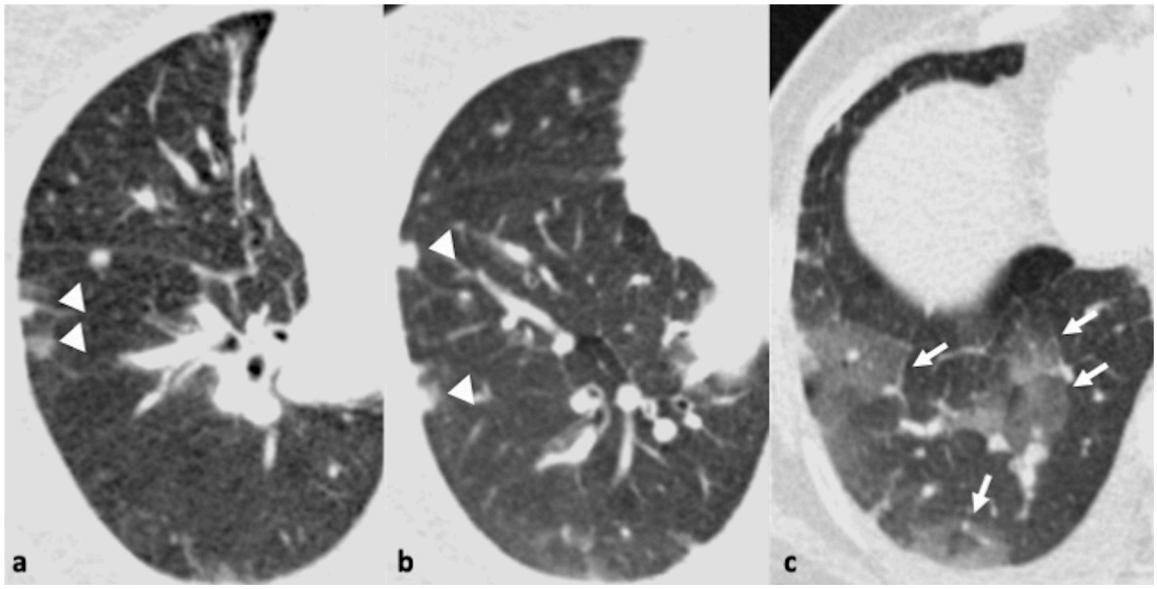

Fig. 5. 64-year-old male with confirmed rhinovirus infection who presented with sore throat and cough with. 5a-c. Axial thin section CT scan demonstrates a few nodules (arrowheads, a, b) and areas of ground glass opacity (arrows, c) in the right lower lobe. Bronchial wall thickening and mild mosaicism is also noted in the left lung base, corroborating small airway inflammation.

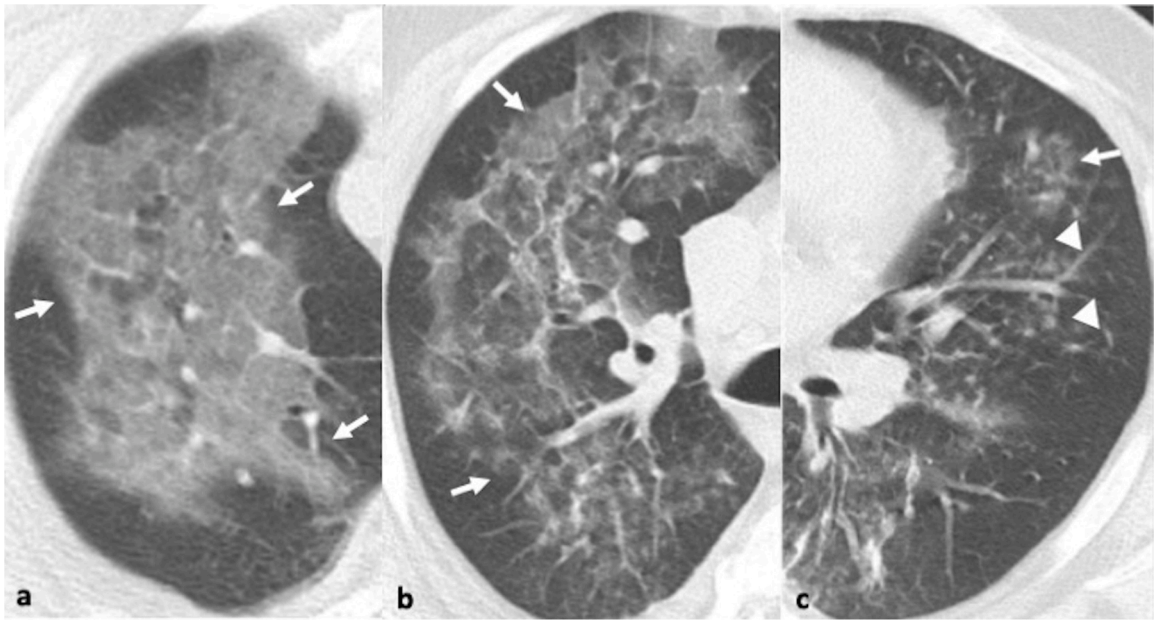

Fig. 6. 47-year-old male with pneumonia due to human metapneumovirus. 6a-c. Axial CT images in the right apical region and right and left mid zone reveal three coexisting patterns: ground glass opacity (arrows, a-c), reticular changes and ill-defined centrilobular nodules (arrowheads, c).

7.5. Human metapneumovirus

Human metapneumovirus (hMPV), first discovered in 2001, is a paramyxovirus that has emerged as an important worldwide cause of lower respiratory tract infections [29]. It is molecularly similar to RSV and parainfluenza virus and shows similar seasonality of outbreaks in winter and spring [13,14]. It most commonly causes upper and lower respiratory tract infections in children, but can also cause pneumonia in adults, particularly in the elderly with cardiopulmonary disease, as well as in immunocompromised populations. In adults, hMPV typically accounts for 2–5 % of CAP, although this percentage can be much higher in hospitalized patients during years with larger outbreaks [42,63–65].

The histological patterns in hMPV pneumonia reflect the radiological appearances and include necrotizing bronchiolitis that evolves to chronic bronchiolitis, acute or organizing DAD and alveolar haemorrhage [65].

Accordingly, bronchial wall thickening, GGOs, and ill-defined centrilobular nodules were the commonest CT findings for hMPV pneumonia in the largest retrospective study of 251 patients with confirmed hMPV and without other pathogen identified [66] (Fig. 6). Macronodules and consolidation were observed in <50 % of patients [66]. In a small study of 10 patients with hMPV pneumonia, the CT findings demonstrated a more asymmetric distribution compared to RSV-pneumonia which presents with more symmetrical involvement [67].

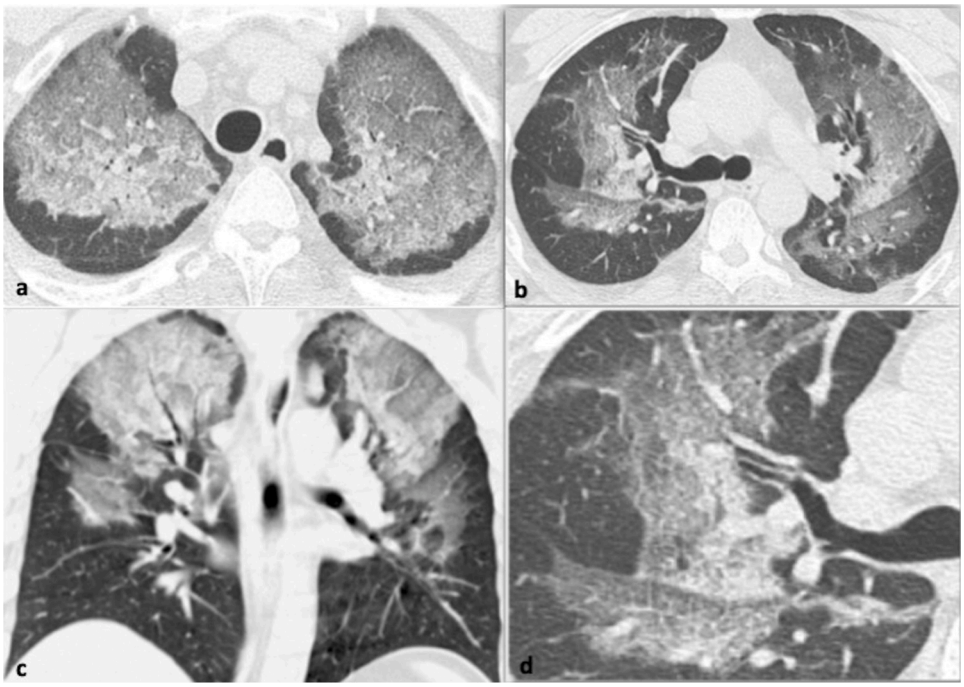

Fig. 7. 31-year-old male with pneumonia due to MERS coronavirus who presented with cough and sputum. 7a-c. Axial and coronal CT images show bilateral symmetrical ground glass opacity with an upper and mid zone distribution. 7d. Small field of view in the right upper lobe at the level of the carina demonstrates a crazy-paving pattern.

7.6. Coronavirus

Coronoviruses are enveloped single-stranded RNA viruses member of the Betacoronavirus genus belonging to the Coronaviridae family. Several strains cause respiratory infections, including the common cold during winter months, but outbreaks throughout the year have been reported [13,14]. In 2002 and 2012, two outbreaks of coronavirus infections occurred by severe acute respiratory syndrome coronavirus (SARS-CoV-1) and Middle East respiratory syndrome coronavirus (MERS-CoV) respectively with the clinical presentation of rapidly progressive pneumonia [68,69].

The histological examination of the lungs in SARS and MERS have similarities showing DAD, pulmonary oedema, and hyaline membrane formation, indicative of acute respiratory distress syndrome (ARDS). Similarly, the imaging features of SARS and MERS may overlap. The initial chest x-ray will be abnormal in up to 80 % of patients with SARS and 83 % of patients with MERS [70]. The initial radiographic appearance in SARS frequently shows ill-defined peripherally distributed areas of airspace opacification in the lower lung zones. The majority of patients will show progressive multifocal consolidation over a course of 6–12 days. CT frequently shows patchy areas of ground glass opacity and consolidation (Fig. 7). The presence of bilateral confluent diffuse airspace opacities, similar to the findings of ARDS, involvement of four or more lung zones, bilateral lung involvement, and progressive worsening of airspace consolidation on chest imaging more than 12 days after symptom onset, despite treatment, are associated with unfavourable outcomes [70].

The radiographic appearance in patients with MERS will show most commonly multifocal airspace opacities in the lower lung zones. MERS pneumonia at CT typically demonstrates bibasilar peripheral predominant ground glass opacities; however, isolated consolidation, interlobular septal thickening, and pleural effusion are not uncommon, observed in 20–33 % of MERS pneumonia [71].

7.7. Novel coronovirus 19

In December 2019, in Wuhan Province in China, a new coronavirus was identified as the pathogen of this disease, SARS-CoV-2 (severe acute respiratory syndrome coronavirus 2), causing coronavirus disease 2019 (Covid-19). The new virus has globally spread and in March 2020 the Covid-19 outbreak was declared as a pandemic by the WHO.

Transmission seems to be similar to that of other coronaviruses [72]. Patients are infectious for up to two days before the onset of symptoms and remain so for 10 days after symptoms onset in mild to moderate disease and for up to 20 days in severe Covid-19 illness [3]. This relatively long infectious period in addition to the fact that many patients may be completely asymptomatic plays an important role in the rapid transmission of the virus.

The predominant laboratory abnormalities include the elevation of inflammatory markers, such as C-reactive protein, lactate dehydrogenase, and the erythrocyte sedimentation rate. Additionally, lymphopenia is consistently present in more than 40 % of patients [73].

Covid-19 may range from asymptomatic disease to fatal multiorgan failure, depending on patients' age, comorbidities and host immune response [74]. The commonest symptoms at onset of the disease include fever, cough, anosmia, dyspnoea and fatigue. In more severe cases of the disease patients develop pneumonia, ARDS (usually developing after 6–7 days of symptoms onset), kidney failure, hypercoagulation disorder and embolic episodes, cytokine release syndrome, septic shock and multi-organ failure. The histopathological findings of acute alveolar damage in Covid-19 pneumonia are similar to those described in SARS-CoV-1 and MERS-CoV with similarities in the pathogenesis and the mechanisms of tissue damage and inflammatory response [75].

In the very early course of the disease imaging findings may be normal. The chest x-ray is typically the first-line imaging modality; however, it is of limited sensitivity and may be normal in the early phase. Chest x-rays can be useful in the follow-up of hospitalized patients monitoring the progression or regression of the disease. In those Covid-19 cases requiring hospitalization, an abnormal chest x-ray has been reported in 69 % of the cases at the initial time of admission, and 80

Fig. 8. 61-year-old male with confirmed Covid-19 pneumonia. Series of chest x-rays show the progressive radiographic changes. 8a. Peripheral distribution of the airspace opacities in day 5 of admission (arrows, a). 8b, c. Radiographic progression with diffuse bilateral involvement of the lungs in day 8 (b) and 10 of admission (c).

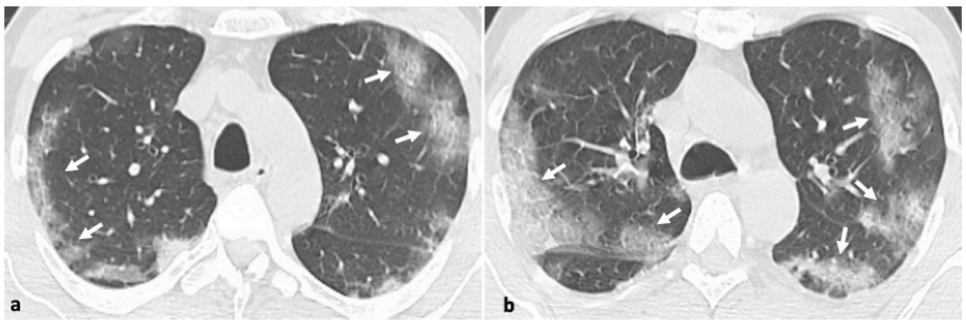

Fig. 9. 51-year-old male with confirmed Covid-19 pneumonia. 9a, b. Axial CT images show typical CT appearances with bilateral peripheral ground glass opacities (arrows).

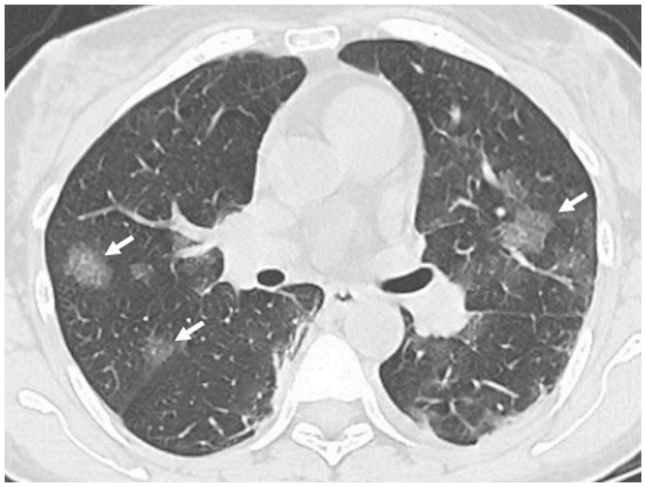

Fig. 10. 59-year-old male with confirmed Covid-19 pneumonia. Axial CT image shows nodular round ground glass discrete opacities bilaterally (arrows).

% had radiographic abnormalities sometime during hospitalization [76]. Chest radiographic abnormalities include ground-glass opacities, coarse horizontal linear opacities, and consolidation [73,76]. These are more likely to be peripheral and in the lower zones, but the whole lung can be involved (Fig. 8a–c).

CT is more sensitive than chest x-ray and shows characteristic imaging patterns in the different stages of the disease [77–79]. In the early stage (0–4 days) the CT imaging findings may be normal or show ground-glass opacities which is the most common finding and has been suggested as the hallmark of Covid-19. Distribution is usually multifocal, bilateral peripheral and posterior (Fig. 9a, b). The presence of typically nodular (round or oval) ground glass opacities (Fig. 10) may suggest the diagnosis and should alert the radiologist to the possibility of Covid-19 infection [80,81]. Another typical finding described in the affected area of ground-glass opacification is pulmonary vascular enlargement which plays a potential diagnostic role for Covid-19. Bai and colleagues have shown that the CT regional pulmonary vascular enlargement was significantly associated with Covid-19 [82]. In the progressive stage (5–8 days), the typical appearance is increased ground glass opacification often combined with thickened interlobular and intralobular lines (crazy paving pattern) (Fig. 11 a). Areas of consolidation is the most common finding in the peak stage (9–13 days). Atypical findings include mediastinal lymphadenopathy and pleural effusions [75]. In the absorption stage (>14 days) traction bronchiectasis and fibrotic bands can be seen (Fig. 11b) with complete or almost complete resolution of abnormalities at one month or beyond.

Different studies have also shown the potential role of CT in predicting the severity of the disease [83,84]. A CT severity score estimating of the percentage of Covid-19 lung involvement by visual assessment can help identify patients with severe forms of Covid-19 and better triage patients [83,84].

8. Selected DNA viruses

8.1. Adenovirus

Adenovirus is a double-stranded DNA virus. Adenovirus pneumonia is rare in healthy individuals [85], while occurs commonly in immunocompromised hosts including patients who have received organ and bone marrow transplants [86,87]. Adenovirus infections can occur throughout the year. Outbreaks of adenovirus-associated respiratory disease have been more common in the late winter, spring, and early summer [13,14].

Clinically, respiratory involvement in non-severe adenovirus infection includes a spectrum of upper and lower respiratory tract manifestations such as rhinitis and conjunctivitis, pharyngitis, tracheitis and

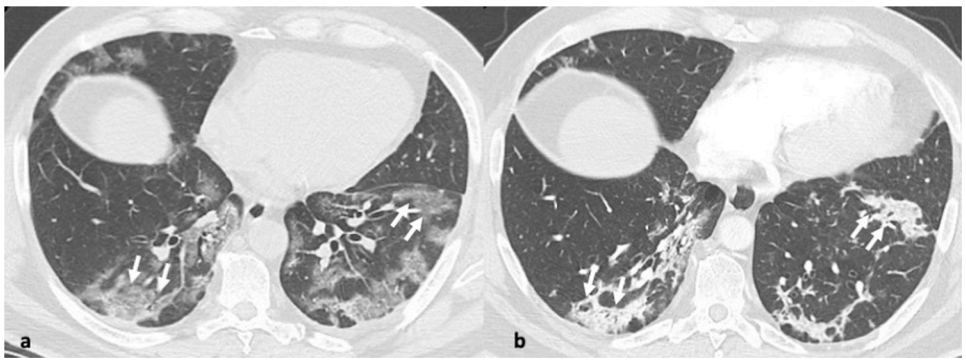

Fig. 11. 59-year-old man with confirmed Covid-19 pneumonia who presented with chest pain, cough, and fever. 11a. Axial CT image shows ground glass opacity and a crazy-paving pattern with peripheral distribution (arrows). 11b. In the same patient, axial CT image 5 days later shows at the same level, progression to organizing consolidation (arrows) and some fibrotic bands indicative of the late peak and early absorption stage.

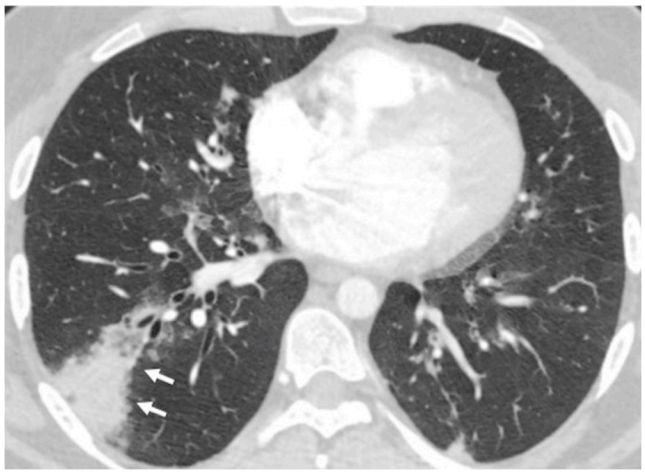

Fig. 12. 42-year-old male with fever following bone marrow transplantation. Adenovirus was the only pathogen recovered from respiratory secretions. Axial CT image shows segmental consolidation with mild surrounding ground glass in the right lower lobe (arrows). A small subpleural focus of consolidation is also seen.

bronchitis. In mild disease, findings of interstitial inflammatory cell inflammation are present while in severe pneumonia, haemorrhage and DAD are the predominant histological patterns. Chest x-ray findings may be normal in the early phase and show bilateral or unilateral parenchymal opacities with infective progression. The most common finding on CT is consolidation with or without ground glass opacity with subpleural and peribronchovascular predisposition as shown in a study of 104 immunocompetent patients with adenovirus pneumonia [88]. Less often septal thickening and nodules may also be present [88,89]. As severe adenovirus pneumonia may manifest as focal consolidation, adenovirus is the only virus known to cause focal or lobar consolidation resembling bacterial pneumonia [88,90] (Fig. 12).

8.2. *Herpes simplex virus*

Herpes simplex virus (HSV) includes two types, HSV-1 and HSV-2 and belongs to the alphaherpesvirus subfamily of herpesviruses, sharing the same basic structural features. No seasonality has been demonstrated for HSV-1 infection but case clusters are reported sporadically throughout the year [13,14]. HSV-1 is the type most commonly associated with respiratory infection. Interestingly, isolation of HSV in lower respiratory tract secretions has been reported in patients with ARDS and in mechanically ventilated patients in general and this has been associated with poor prognosis [91,92]. The histopathological pattern of HSV pulmonary infection is of DAD consisting of interstitial lymphocytic infiltration, alveolar haemorrhage and hyaline membrane formation [93].

Radiographic findings include lung air-space opacification, predominantly with focal or more extensive bilateral distribution [94]. The most common CT patterns of pulmonary abnormalities identified in HSV pneumonia are areas of diffuse or multifocal ground glass opacity, multifocal peribronchial consolidations and interlobular septal thickening [95,96].

8.3. *Varicella-Zoster virus*

Varicella-Zoster virus (VZV) is a double-stranded DNA virus and a member of

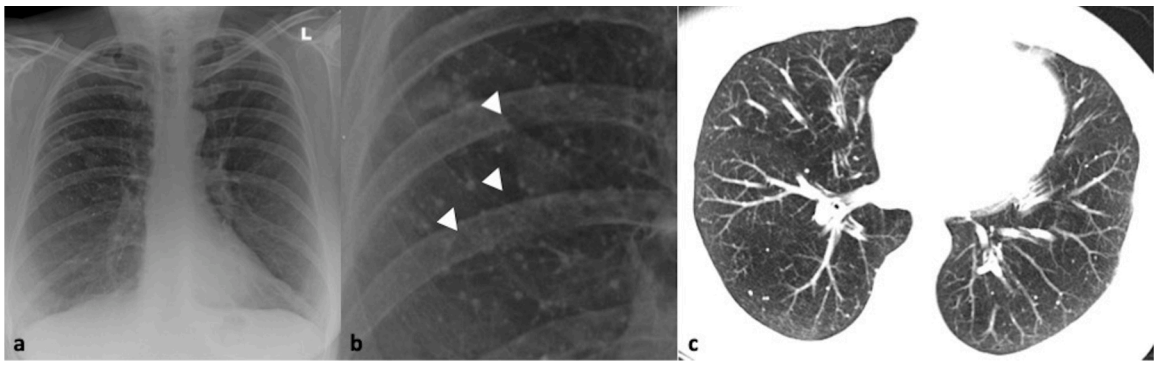

Fig. 13. 35-year-old male with healed varicella-zoster infection. 13a, b. Chest x-ray and close-up view shows multiple, bilateral and randomly distributed tiny calcified nodules (arrowheads). 13c. Axial CT image confirms the findings of the chest radiograph.

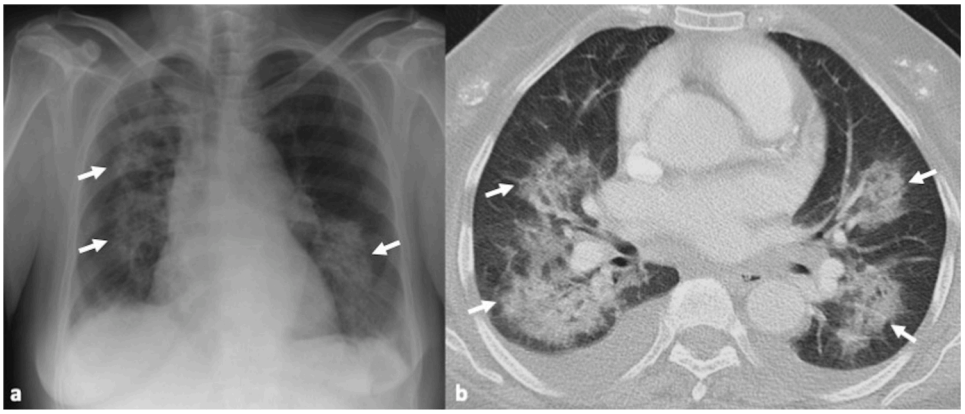

Fig. 14. 67-year-old female patient with pneumonia due to cytomegalovirus following kidney transplantation. 14a. Chest x-ray shows bilateral air-space opacification (arrows). 14b. Axial CT image shows the bilateral patchy areas of consolidation and ground glass opacity (arrows) associated with bilateral pleural effusions.

the Herpesviridae family that typically causes outbreaks of a highly contagious childhood disease (Varicella – "chickenpox") in late winter and early spring months in temperate regions [13,14]. The diagnosis of varicella infection usually can be established on the basis of clinical findings (rash, pulmonary symptoms, and history of contact with a patient with chickenpox). Clinical manifestations of VZV pneumonia are non-specific and include fever, cough, dyspnoea, pleuritic chest pain and haemoptysis. Histologic features of pneumonitis associated with chickenpox and zoster include an interstitial mononuclear inflammatory infiltrate associated with features of DAD including intraalveolar proteinaceous exudate, hyaline membrane formation, and type II cell hyperplasia.

Chest radiographic findings of varicella-zoster virus pneumonia consist of multiple scattered 5–10-mm ill-defined nodules that may be confluent (Fig. 13a, b). The nodules may persist for several months and can calcify and persist as numerous, well-defined, randomly scattered, 2−3 mm dense calcifications. CT findings of varicella-zoster pneumonia include nodules, nodules with surrounding ground-glass attenuation (halo sign), patchy ground glass opacities and coalescence of nodules; the disappearance of these features on CT corresponds to healing of skin lesion in patients after antiviral chemotherapy [97]. Similarly, to the radiographic appearances, nodules may calcify and persist as well-defined, randomly scattered, 2−3 mm densely calcified nodules (Fig. 13c).

8.4. Cytomegalovirus

Cytomegalovirus (CMV) belongs to the gammaherpesvirus subfamily of the herpes viruses. No seasonal patterns of CMV infection have been described. CMV respiratory manifestations are rare in healthy hosts in contrast to immunocompromised patients. In allogeneic bone marrow transplant recipient CMV is the most common infectious cause of interstitial pneumonia and is associated with a high fatality rate if left untreated. The risk of CMV pneumonia is greatest 30–90 days after bone marrow transplant [98,99].

Histological features of CMV pneumonia consist of areas of acute interstitial pneumonia, DAD and haemorrhage. Chest x-ray is the first imaging technique performed with variable radiographic manifestations; reticular or reticulonodular patterns, ground glass opacity, consolidative findings, or a combination of these patterns prevail [100]. The CT features provide additional information and reflect on the underlying histological pattern. At CT small centrilobular nodules, bilateral ground glass opacity and consolidation predominate [101–103] (Fig. 14). CMV pneumonia is an acquired immunodeficiency syndrome (AIDS) defining illness; notably in this sub-population masses and mass-like infiltrates are more common than in patients without AIDS [101,104].

8.5. Hantavirus

Hantaviruses belong to the Bunyavirus family which encompasses a number of genetically diverse viruses including the "Sin Nombre" virus, the hantavirus responsible for an outbreak of severe pulmonary disease in the southwestern United States in 1993 [105]. Hantaviruses can cause severe, often fatal, respiratory manifestations, the so-called "Hantavirus Pulmonary Syndrome (HPS)". Presentation of HPS begins with non-specific symptoms. Physical examination may demonstrate petechiae, leg oedema and mild dyspnoea. It progresses to development of mild, non-productive cough and progressive dyspnoea and finally to pulmonary oedema resulting from leakage of high-protein fluid into the alveoli, cardiac dysfunction and shock [106]. Histologically, hantavirus pneumonia consists of the exudative and proliferative phase of DAD.

The chest x-ray appearance may be unremarkable in the early phase with features of interstitial oedema with the progression of the infection [107]. The CT features consist of extensive bilateral ground glass opacity with mid and lower zone predominance, a few slightly thickened interlobular septa and poorly defined small nodules, bronchial wall thickening and small bilateral pleural effusions [108].

9. Conclusion

Viral pathogens are responsible for a significant cause of death worldwide in healthy and immunocompromised hosts. Although our knowledge of the different organisms has increased over the last decades, the diagnosis still strongly relies on clinical suspicion. However, combining imaging findings with relevant clinical and epidemiological features can enable radiologists and clinicians to significantly narrow the differential diagnosis. Radiological findings can influence early treatment decisions, before the results of molecular tests are available guiding clinical management and improving patient outcomes.

Declaration of Competing Interest

The authors report no declarations of interest.

References

[1] J.R. Fears, The plague under Marcus Aurelius and the decline and fall of the Roman Empire, Infect. Dis. Clin. North Am. 18 (March (1)) (2004) 65–77, https://doi.org/10.1016/s0891-5520(03)00089-8.
[2] A. Suzuki, Smallpox and the epidemiological heritage of modern Japan: towards a total history, Med. Hist. 55 (July (3)) (2011) 313–318, https://doi.org/10.1017/s0025727300005329.
[3] Centers for Disease Control and Prevention, Past pandemics, Available at: https://www.cdc.gov/flu/pandemic-resources/basics/past-pandemics.html (Accessed 09 October 2020).

[4] D. Kobasa, Y. Kawaoka, Emerging influenza viruses: past and present, Curr. Mol. Med. 5 (December (8)) (2005) 791–803, https://doi.org/10.2174/156652405774962281.
[5] V.M. Corman, D. Muth, D. Niemeyer, C. Drosten, Hosts and sources of endemic human coronaviruses, Adv. Virus Res. 100 (2018) 163–188, https://doi.org/10.1016/bs.aivir.2018.01.001.
[6] O. Ruuskanen, E. Lahti, L.C. Jennings, D.R. Murdoch, Viral pneumonia, Lancet 377 (April (9773)) (2011) 1264–1275, https://doi.org/10.1016/s0140-6736(10)61459-6.
[7] L.C. Jennings, T.P. Anderson, K.A. Beynon, et al., Incidence and characteristics of viral community-acquired pneumonia in adults, Thorax 63 (January (1)) (2008) 42–48, https://doi.org/10.1136/thx.2006.075077.
[8] J. Johnstone, S.R. Majumdar, J.D. Fox, T.J. Marrie, Human metapneumovirus pneumonia in adults: results of a prospective study, Clin. Infect. Dis. 46 (February 15 (4)) (2008) 571–574, https://doi.org/10.1086/526776.
[9] A. de Roux, M.A. Marcos, E. Garcia, et al., Viral community-acquired pneumonia in non-immunocompromised adults, Chest 125 (April (4)) (2004) 1343–1351.
[10] M.A. Marcos, M. Camps, T. Pumarola, et al., The role of viruses in the aetiology of community-acquired pneumonia in adults, Antivir. Ther. 11 (3) (2006) 351–359.
[11] E. Vakil, S.E. Evan, Viral pneumonia in patients with hematologic malignancy or hematopoietic stem cell transplantation, Clin. Chest Med. 38 (March (1)) (2017) 97–111, https://doi.org/10.1016/j.ccm.2016.11.002.
[12] S. Jain, Epidemiology of viral pneumonia, Clin. Chest Med. 38 (March (1)) (2017) 1–9, https://doi.org/10.1016/j.ccm.2016.11.012.
[13] R.H.M. Price, C. Graham, S. Ramalingam, Association between viral seasonality and meteorological factors, Sci. Rep. 9 (2019) 929, https://doi.org/10.1038/s41598-018-37481-y.
[14] P.D.S. Stewart, Seasonality and selective trends in viral acute respiratory tract infections, Med. Hypotheses 86 (2016) 104–119, https://doi.org/10.1016/j.mehy.2015.11.005.
[15] J. Shaman, M. Kohn, Absolute humidity modulates influenza survival, transmission, and seasonality, Proc. Natl. Acad. Sci. U. S. A. 106 (March 3 (9)) (2009) 3243–3248, https://doi.org/10.1073/pnas.0806852106.
[16] R.F. Grais, J.H. Ellis, A. Kress, G.E. Glass, Modeling the spread of annual influenza epidemics in the U.S.: the potential role of air travel, Health Care Manage. Sci. 7 (May (2)) (2004) 127–134, https://doi.org/10.1023/b:hcms.0000020652.38181.da.
[17] L.S. Souza, E.A. Ramos, F.M. Carvalho, et al., Viral respiratory infections in young children attending day care in urban Northeast Brazil, Pediatr. Pulmonol. 35 (March (3)) (2003) 184–191, https://doi.org/10.1002/ppul.10194.
[18] J.J. Cannell, R. Vieth, J.C. Umhau, et al., Epidemic influenza and vitamin D, Epidemiol. Infect. 134 (December (6)) (2006) 1129–1140, https://doi.org/10.1017/s0950268806007175.
[19] T.M. Mäkinen, R. Juvonen, J. Jokelainen, et al., Cold temperature and low humidity are associated with increased occurrence of respiratory tract infections, Respir. Med. 103 (March (3)) (2009) 456–462, https://doi.org/10.1016/j.rmed.2008.09.011.
[20] J. Tamerius, M.I. Nelson, S.Z. Zhou, C. Viboud, M.A. Miller, W.J. Alonso, Global influenza seasonality: reconciling patterns across temperate and tropical regions, Environ. Health Perspect. 119 (April (4)) (2011) 439–445, https://doi.org/10.1289/ehp.1002383.
[21] Y.F. Liu, Y. Gao, M.F. Chen, B. Cao, X.H. Yang, L. Wei, Etiological analysis and predictive diagnostic model building of community-acquired pneumonia in adult outpatients in Beijing, China, BMC Infect. Dis. 309 (July (13)) (2013), https://doi.org/10.1186/1471-2334-13-309.
[22] D.M. Musher, I.L. Roig, G. Cazares, C.E. Stager, N. Logan, H. Safar, Can an etiologic agent be identified in adults who are hospitalized for community-acquired pneumonia: results of a one-year study, J. Infect. 67 (July (1)) (2013) 11–18, https://doi.org/10.1016/j.jinf.2013.03.003.
[23] J.A. McCullers, The co-pathogenesis of influenza viruses with bacteria in the lung, Nat. Rev. Microbiol. 12 (April (4)) (2014) 252–262, https://doi.org/10.1038/nrmicro3231.
[24] D.M. Morens, J.K. Taubenberger, A.S. Fauci, Predominant role of bacterial pneumonia as a cause of death in pandemic influenza: implications for pandemic influenza preparedness, J. Infect. Dis. 198 (October 1 (7)) (2008) 962–970, https://doi.org/10.1086/591708.
[25] E. Bautista, T. Chotpitayasunondh, Z. Gao, et al., Writing Committee of the WHO Consultation on Clinical Aspects of Pandemic (H1N1) 2009 Influenza. Clinical aspects of pandemic 2009 influenza A (H1N1) virus infection, N. Engl. J. Med. 362 (May 6 (18)) (2010) 1708–1719, https://doi.org/10.1056/nejmra1000449.
[26] J.K. Louie, M. Acosta, K. Winter, et al., Factors associated with death or hospitalization due to pandemic 2009 influenza A(H1N1) infection in California, JAMA 302 (November (17)) (2009) 1896–1902, https://doi.org/10.1001/jama.2009.1583.
[27] A. Kumar, R. Zarychanski, R. Pinto, et al., Critically ill patients with 2009 influenza A(H1N1) infection in Canada, JAMA 302 (November (17)) (2009) 1872–1879, https://doi.org/10.1001/jama.2009.1496.
[28] D.R. Murdoch, K.L. O'Brien, J.A.G. Scott, et al., Breathing new life into pneumonia diagnostics, J. Clin. Microbiol. 47 (November (11)) (2009) 3405–3408, https://doi.org/10.1128/jcm.01685-09.
[29] B.G. van den Hoogen, J.C. de Jong, J. Groen, et al., A newly discovered human pneumovirus isolated from young children with respiratory tract disease, Nat. Med. 7 (June (6)) (2001) 719–724, https://doi.org/10.1038/89098.
[30] N. Johansson, M. Kalin, A. Tiveljung-Lindell, C.G. Giske, J. Hedlund, Etiology of community-acquired pneumonia: increased microbiological yield with new diagnostic methods, Clin. Infect. Dis. 50 (January 15 (2)) (2010) 202–209, https://doi.org/10.1086/648678.
[31] J.M. Miller, M.J. Binnicker, S. Campbell, et al., A guide to utilization of the microbiology laboratory for diagnosis of infectious diseases: 2018 update by the Infectious Diseases Society of America and the American Society for Microbiology, Clin. Infect. Dis. 67 (August (6)) (2018) e1–e94, https://doi.org/10.1093/cid/ciy381.
[32] A.W. Graffelman, F.E.J.A. Willemssen, H.M. Zonderland, A.K. Neven, A.C. M. Kroes, P.J. van den Broek, Limited value of chest radiography in predicting aetiology of lower respiratory tract infection in general practice, Br. J. Gen. Pract. 58 (February (547)) (2008) 93–97, https://doi.org/10.3399/bjgp08x264054.
[33] B.M. Diederen, M.M. Van Der Eerden, F. Vlaspolder, W.G. Boersma, J. A. Kluytmans, M.F. Peeters, Detection of respiratory viruses and Legionella spp. by real-time polymerase chain reaction in patients with community acquired pneumonia, Scand. J. Infect. Dis. 41 (July (1)) (2009) 45–50, https://doi.org/10.1080/00365540802448799.
[34] E.A. Kim, K.S. Lee, S.L. Primack, et al., Viral pneumonias in adults: radiologic and pathologic findings, Radiographics 22 (2002) S137–S149, https://doi.org/10.1148/radiographics.22.suppl_1.g02oc15s137.
[35] J.K. Taubenberger, D.M. Morens, The pathology of influenza virus infections, Annu. Rev. Pathol. 3 (2008) 499–522, https://doi.org/10.1146/annurev.pathmechdis.3.121806.154316.
[36] G. Aviram, A. Bar-Shai, J. Sosna, et al., H1N1 influenza: initial chest radiographic findings in helping predict patient outcome, Radiology 255 (April (1)) (2010) 252–259, https://doi.org/10.1148/radiol.10092240.
[37] A.M. Ajlan, B. Quiney, S. Nicolaou, N.L. Müller, Swine-origin influenza A (H1N1) viral infection: radiographic and CT findings, AJR 193 (December (6)) (2009) 1494–1499, https://doi.org/10.2214/ajr.09.3625.
[38] W.T.Jr. Miller, T.J. Mickus, E.Jr. Barbosa, et al., CT of viral lower respiratory tract infections in adults: comparison among viral organisms and between viral and bacterial infections, AJR 197 (November (5)) (2011) 1088–1095, https://doi.org/10.2214/ajr.11.6501.
[39] Y. Yuan, X.F. Tao, Y.X. Shi, S.Y. Liu, J.Q. Chen, Initial HRCT findings of novel influenza A (H1N1) infection, influenza other respir, Viruses 6 (November (6)) (2012) e114–e119, https://doi.org/10.1111/j.1750-2659.2012.00368.x.
[40] Q. Wang, Z. Zhang, Y. Shi, Y. Jiang, Emerging H7N9 influenza A (novel reassortant avian-origin) pneumonia: radiologic findings, Radiology 268 (September (3)) (2013) 882–889, https://doi.org/10.1148/radiol.13130988.
[41] A. Oikonomou, N.L. Müller, S. Nantel, Radiographic and high-resolution CT findings of influenza virus pneumonia in patients with hematologic malignancies, AJR 181 (August (2)) (2003) 507–511, https://doi.org/10.2214/ajr.181.2.1810507.
[42] J.X. Qu, L. Gu, Z.H. Pu, et al., Beijing Network for Adult Community-Acquired Pneumonia (BNACAP), 2015. Viral etiology of community-acquired pneumonia among adolescents and adults with mild or moderate severity and its relation to age and severity, BMC Infect. Dis. 89 (February (15)) (2015), https://doi.org/10.1186/s12879-015-0808-0.
[43] W.H. Self, D.J. Williams, Y. Zhu, et al., Respiratory viral detection in children and adults: comparing asymptomatic controls and patients with community-acquired pneumonia, J. Infect. Dis. 213 (February 15 (4)) (2016) 584–591, https://doi.org/10.1093/infdis/jiv323.
[44] W.G. Nichols, L. Corey, T. Gooley, C. Davis, M. Boeckh, Parainfluenza virus infections after hematopoietic stem cell transplantation: risk factors, response to antiviral therapy, and effect on transplant outcome, Blood 98 (August 1 (3)) (2001) 573–578, https://doi.org/10.1182/blood.v98.3.573.
[45] P.E. Ferguson, T.C. Sorrell, K. Bradstock, P. Carr, N.M. Gilroy, Parainfluenza virus type 3 pneumonia in bone marrow transplant recipients: multiple small nodules in high- resolution lung computed tomography scans provide a radiological clue to diagnosis, Clin. Infect. Dis. 48 (April 1 (7)) (2009) 905–909, https://doi.org/10.1086/597297.
[46] T. Herbst, V.M. Van Deerlin, W.T.Jr. Miller, The CT appearance of lower respiratory infection due to parainfluenza virus in adults, AJR 201 (September (3)) (2013) 550–554, https://doi.org/10.2214/ajr.12.9613.
[47] E.L. Gasparetto, D.L. Escuissato, E. Marchiori, S. Ono, R.L. Frare e Silva, N. L. Müller, High-resolution CT findings of respiratory syncytial virus pneumonia after bone marrow transplantation, AJR 182 (May (5)) (2004) 1133–1137, https://doi.org/10.2214/ajr.182.5.1821133.
[48] T. Franquet, N.L. Müller, A. Giménez, S. Martínez, M. Madrid, P. Domingo, Infectious pulmonary nodules in immunocompromised patients: usefulness of computed tomography in predicting their etiology, J. Comput. Assist. Tomogr. 27 (July-August (4)) (2003) 461–468, https://doi.org/10.1097/00004728-200307000-00001.
[49] E.J. Anaissie, T.H. Mahfouz, T. Aslan, et al., The natural history of respiratory syncytial virus infection in cancer and transplant patients: implications for management, Blood 103 (March 1 (5)) (2004) 1611–1617, https://doi.org/10.1182/blood-2003-05-1425.
[50] E. Whimbey, S. Ghosh, Respiratory syncytial virus infections in immunocompromised adults, Curr. Clin. Top. Infect. Dis. 20 (2000) 232–255.
[51] R. Pickles, J. DeVincenzo, RSV and its propensity for causing bronchioloitis, J. Pathol. 235 (January (2)) (2015) 266–267, https://doi.org/10.1002/path.4462.
[52] S. Kern, M. Uhl, R. Berner, T. Schwoerer, M. Langer, Respiratory syncytial virus infection of the lower respiratory tract: radiological findings in 108 children, Eur. Radiol. 11 (2001) 2581–2584, https://doi.org/10.1007/s003300100887.
[53] D. Niles, B. Larsen, A. Balaji, et al., Retrospective review of clinical and chest X-Ray findings in children admitted to a community hospital for respiratory

syncytial virus infection, Clin. Pediatr. (Phila) 57 (December (14)) (2018) 1686–1692, https://doi.org/10.1177/0009922818795902.
[54] F.J. Sorvillo, S.F. Huie, M.A. Strassburg, A. Butsumyo, W.X. Shandera, S. L. Fannin, An outbreak of respiratory syncytial virus pneumonia in a nursing home for the elderly, J. Infect. 9 (November (3)) (1984) 252–256, https://doi.org/10.1016/s0163-4453(84)90530-9.
[55] J.L. Mayer, N. Lehners, G. Egerer, H.U. Kauczor, C.P. Heußel, CT-morphological characterization of respiratory syncytial virus (RSV) pneumonia in immune-compromised adults, Rofo 186 (July (7)) (2014) 686–692, https://doi.org/10.1055/s-0033-1356353.
[56] S.H. Choi, S.B. Hong, T. Kim, et al., Clinical and molecular characterization of rhinoviruses A, B, and C in adult patients with pneumonia, J. Clin. Virol. 63 (2015) 70–75, https://doi.org/10.1016/j.jcv.2014.12.016.
[57] S. Mermond, A. Berlioz-Arthaud, M. Estivals, F. Baumann, H. Levenes, P. M. Martin, Aetiology of community-acquired pneumonia in hospitalized adult patients in New Caledonia, Trop. Med. Int. Health 15 (December (12)) (2010) 1517–1524, https://doi.org/10.1111/j.1365-3156.2010.02653.x.
[58] A.S. Monto, The seasonality of rhinovirus infections and its implications for clinical recognition, Clin. Ther. 24 (December (12)) (2002) 1987–1997, https://doi.org/10.1016/s0149-2918(02)80093-5.
[59] T.E. Minor, E.C. Dick, J.W. Baker, J.J. Ouellette, M. Cohen, C.E. Reed, Rhinovirus and influenza type A infections as precipitants of asthma, Am. Rev. Respir. Dis. 113 (February (2)) (1976) 149–153, https://doi.org/10.1164/arrd.1976.113.2.149.
[60] S.B. Greenberg, M. Allen, J. Wilson, R.L. Atmar, Respiratory viral infections in adults with and without chronic obstructive pulmonary disease, Am. J. Respir. Crit. Care Med. 162 (July (1)) (2000) 167–173, https://doi.org/10.1164/ajrccm.162.1.9911019.
[61] J.L. Kennedy, R.B. Turner, T. Braciale, P.W. Heymann, L. Borish, Pathogenesis of rhinovirus infection, Curr. Opin. Virol. 2 (June (3)) (2012) 287–293, https://doi.org/10.1016/j.coviro.2012.03.008.
[62] S.H. Choi, J.W. Huh, S.B. Hong, et al., Clinical characteristics and outcomes of severe rhinovirus-associated pneumonia identified by bronchoscopic bronchoalveolar lavage in adults: comparison with severe influenza virus-associated pneumonia, J. Clin. Virol. 62 (2015) 41–47, https://doi.org/10.1016/j.jcv.2014.11.010.
[63] J. Stockton, I. Stephenson, D. Fleming, M. Zambon, Human metapneumovirus as a cause of community-acquired respiratory illness, Emerg. Infect. Dis. 8 (September (9)) (2002) 897–901, https://doi.org/10.3201/eid0809.020084.
[64] E.E. Walsh, D.R. Peterson, A.R. Falsey, Human metapneumovirus infections in adults: another piece of the puzzle, Arch. Intern. Med. 168 (December 8 (22)) (2008) 2489–2496, https://doi.org/10.1001/archinte.168.22.2489.
[65] K.C. Sumino, E. Agapov, R.A. Pierce, et al., Detection of severe human metapneumovirus infection by real-time polymerase chain reaction and histopathological assessment, J. Infect. Dis. 192 (September 15 (6)) (2005) 1052–1060, https://doi.org/10.1086/432728.
[66] H.J. Koo, H.N. Lee, S.H. Choi, H. Sung, H.J. Kim, K.H. Do, Clinical and Radiologic Characteristics of Human Metapneumovirus Infections in Adults, South Korea, Emerg. Infect. Dis. 25 (January (1)) (2019) 15–24, https://doi.org/10.3201/eid2501.181131.
[67] R. Syha, R. Beck, J. Hetzel, et al., Human metapneumovirus (HMPV) associated pulmonary infections in immunocompromised adults–initial CT findings, disease course and comparison to respiratory-syncytial-virus (RSV) induced pulmonary infections, Eur. J. Radiol. 81 (December (12)) (2012) 4173–4178, https://doi.org/10.1016/j.ejrad.2012.06.024.
[68] R.J. de Groot, S.C. Baker, R.S. Baric, et al., Middle East respiratory syndrome coronavirus (MERS-CoV); announcement of the Coronavirus Study Group, J. Virol. 87 (July (14)) (2013) 7790–7792, https://doi.org/10.1128/jvi.01244-13.
[69] K.L. Hon, C.W. Leung, W.T. Cheng, et al., Clinical presentations and outcome of severe acute respiratory syndrome in children, Lancet 361 (May (9370)) (2003) 1701–1703, https://doi.org/10.1016/s0140-6736(03)13364-8.
[70] K.T. Wong, G.E. Antonio, D.S. Hui, et al., Severe acute respiratory syndrome: radiographic appearances and pattern of progression in 138 patients, Radiology 228 (August (2)) (2003) 401–406, https://doi.org/10.1148/radiol.2282030593.
[71] K.M. Das, E.Y. Lee, M.A. Enani, et al., CT correlation with out- comes in 15 patients with acute Middle East respiratory syndrome coronavirus, AJR 204 (April (4)) (2015) 736–742, https://doi.org/10.2214/ajr.14.13671.
[72] S.A. Lauer, K.H. Grantz, Q. Bi, et al., The incubation period of coronavirus disease 2019 (COVID-19). From publicly reported confirmed cases: estimation and application, Ann. Intern. Med. 172 (May (9)) (2020) 577–582, https://doi.org/10.7326/m20-0504.
[73] A.J. Rodriguez-Morales, J.A. Cardona-Ospina, E. Gutierrez-Ocampo, et al., Clinical, laboratory and imaging features of COVID-19: a systematic review and meta-analysis, Travel Med. Infect. Dis. 34 (2020) 101623, https://doi.org/10.1016/j.tmaid.2020.101623.
[74] W. Cao, T. Li, COVID-19: towards understanding of pathogenesis, Cell Res. 30 (May (5)) (2020) 367–369, https://doi.org/10.1038/s41422-020-0327-4.
[75] K.O. Alsaad, Y.M. Arabi, A.H. Hajeer, Spectrum of histopathological findings in coronavirus disease-19, Middle East respiratory syndrome and severe acute respiratory syndrome, Ann. Thorac. Med. 15 (April- June (2)) (2020) 52–53, https://doi.org/10.4103/atm.atm_105_20.
[76] H.Y.F. Wong, H.Y.S. Lam, A.H. Fong, et al., Frequency and distribution of chest radiographic findings in COVID-19 positive patients, Radiology 296 (August (2)) (2020) E72–E78, https://doi.org/10.1148/radiol.2020201160.
[77] F. Pan, T. Ye, P. Sun, et al., Time course of lung changes on chest CT during recovery from 2019 novel coronavirus (COVID-19) pneumonia, Radiology 295 (June (3)) (2020) 715–721, https://doi.org/10.1148/radiol.2020200370.
[78] Y. Pan, H. Guan, S. Zhou, et al., Initial CT findings and temporal changes in patients with the novel coronavirus pneumonia (2019-nCoV): a study of 63 patients in Wuhan, China, Eur. Radiol. 30 (June (6)) (2020) 3306–3309, https://doi.org/10.1007/s00330-020-06731-x.
[79] J.P. Kanne, Chest CT findings in 2019 novel coronavirus (2019-nCoV) infections from Wuhan, China: key points for the radiologist, Radiology 295 (April (1)) (2020) 16–17, https://doi.org/10.1148/radiol.2020200241.
[80] W. Kong, P.P. Agarwal, Chest imaging appearance of COVID-19 infection, Radiol. Cardiothorac. Imaging. 2 (2020), https://doi.org/10.1148/ryct.2020200028 e200028.
[81] M. Chung, A. Bernheim, X. Mei, et al., CT imaging features of 2019 novel coronavirus (2019-nCoV), Radiology 295 (April (1)) (2020) 202–207, https://doi.org/10.1148/radiol.2020200230.
[82] H.X. Bai, B. Hsieh, Z. Xiong, et al., Performance of radiologists in differentiating COVID-19 from non-COVID-19 viral pneumonia on chest CT, Radiology 296 (August (2)) (2020) E46–E54, https://doi.org/10.1148/radiol.2020200823.
[83] Y. Li, L. Xia, Coronavirus disease 2019 (COVID-19): role of chest CT in diagnosis and management, AJR 214 (June (6)) (2020) 1280–1286, https://doi.org/10.2214/ajr.20.22954.
[84] W. Yang, Q. Cao, L. Qin, X. Wang, Clinical characteristics and imaging manifestations of the 2019 novel coronavirus disease (COVID-19): a multi-center study in Wenzhou city, Zhejiang, China, J. Infect. 80 (April (4)) (2020) 388–393, https://doi.org/10.1016/j.jinf.2020.02.016.
[85] M. Motallebi, B.N. Mukunda, K. Ravakhah, Adenoviral Bronchopneumonia in an immunocompetent adult: computed tomography and pathologic correlations, Am. J. Med. Sci. 325 (May (5)) (2003) 285–287, https://doi.org/10.1097/00000441-200305000-00006.
[86] J.M. Zahradnik, M.J. Spencer, D.D. Porter, Adenovirus infection in the immunocompromised patient, Am. J. Med. 68 (May (5)) (1980) 725–732, https://doi.org/10.1016/0002-9343(80)90262-4.
[87] B.A. Dudding, S.C. Wagner, J.A. Zeller, J.T. Gmelich, G.R. French, F.H. Jr Top, Fatal pneumonia associated with adenovirus type 7 in three military trainees, N. Engl. J. Med. 286 (June (24)) (1972) 1289–1292, https://doi.org/10.1056/nejm197206152862403.
[88] C.K. Park, H. Kwon, J.Y. Park, Thin-section computed tomography findings in 104 immunocompetent patients with adenovirus pneumonia, Acta Radiol. 58 (August (8)) (2017) 937–943, https://doi.org/10.1177/0284185116681039.
[89] S. Chong, K.S. Lee, T.S. Kim, M.J. Chung, M.P. Chung, J. Han, Adenovirus pneumonia in adults: radiographic and high-resolution CT findings in five patients, AJR 186 (May (5)) (2006) 1288–1293, https://doi.org/10.2214/ajr.05.0128.
[90] D. Tan, Y. Fu, J. Xu, et al., Severe adenovirus community-acquired pneumonia in immunocompetent adults: chest radiographic and CT findings, J. Thorac. Dis. 8 (May (5)) (2016) 848–854, https://doi.org/10.21037/jtd.2016.03.38.
[91] G.M. Ong, K. Lowry, S. Mahajan, et al., Herpes simplex type 1 shedding is associated with reduced hospital survival in patients receiving assisted ventilation in a tertiary referral intensive care unit, J. Med. Virol. 72 (January (1)) (2004) 121–125, https://doi.org/10.1002/jmv.10524.
[92] P. Bruynseels, P.G. Jorens, H.E. Demey, et al., Herpes simplex virus in the respiratory tract of critical care patients: a prospective study, Lancet 362 (November (9395)) (2003) 1536–1541, https://doi.org/10.1016/s0140-6736(03)14740-x.
[93] P.G. Ramsey, K.H. Fife, R.C. Hackman, et al., Herpes simplex virus pneumonia: clinical, virologic, and pathologic features in 20 patients, Ann. Intern. Med. 97 (December (6)) (1982) 813–820, https://doi.org/10.7326/0003-4819-97-6-813.
[94] U. Umans, R.P. Golding, S. Duraku, R.A. Manoliu, Herpes simplex virus 1 pneumonia: conventional chest radiograph pattern, Eur. Radiol. 11 (February (6)) (2001) 990–994, https://doi.org/10.1007/s003300000696.
[95] S. Chong, T.S. Kim, E.Y. Cho, Herpes simplex virus pneumonia: high-resolution CT findings, Br. J. Radiol. 83 (July (991)) (2010) 585–589, https://doi.org/10.1259/bjr/51409455.
[96] H. Brodoefel, M. Vogel, D. Spira, et al., Herpes-Simplex-Virus 1 pneumonia in the immunocompromised host: high-resolution CT patterns in correlation to outcome and follow-up, Eur. J. Radiol. 81 (April (4)) (2012) e415–e420, https://doi.org/10.1016/j.ejrad.2011.03.014.
[97] J.S. Kim, C.W. Ryu, S.I. Lee, D.W. Sung, C.K. Park, High-resolution CT findings of varicella-zoster pneumonia, AJR 172 (January (1)) (1999) 113–116, https://doi.org/10.2214/ajr.172.1.9888749.
[98] C.A. Muller, H. Hebart, A. Roos, et al., Correlation of interstitial pneumonia with human cytomegalovirus-induced lung infection and graft-versus-host disease after bone marrow transplantation, Med. Microbiol. Immunol. 184 (October (3)) (1995) 115–121, https://doi.org/10.1007/bf00224347.
[99] S.A. Worthy, J.D. Flint, N.L. Müller, Pulmonary complications after bone marrow transplantation: high-resolution CT and pathologic findings, Radiographics 17 (November-December (6)) (1997) 1359–1371, https://doi.org/10.1148/radiographics.17.6.9397451.
[100] J.F. Olliff, M.P. Williams, Radiological appearances of cytomegalovirus infections, Clin. Radiol. 40 (September (5)) (1989) 463–467, https://doi.org/10.1016/s0009-9260(89)80245-4.
[101] G. McGuinness, J.V. Scholes, S.M. Garay, B.S. Leitman, D.I. McCauley, D. P. Naidich, Cytomegalovirus pneumonitis: spectrum of parenchymal CT findings with pathologic correlation in 21 AIDS patients, Radiology 192 (August (2)) (1994) 451–459, https://doi.org/10.1148/radiology.192.2.8029414.

[102] J.H. Moon, E.A. Kim, K.S. Lee, T.S. Kim, K.J. Jung, J.H. Song, Cytomegalovirus pneumonia: high-resolution CT findings in ten non-AIDS immunocompromised patients, Korean J. Radiol. 1 (April-June (2)) (2000) 73–78, https://doi.org/10.3348/kjr.2000.1.2.73.

[103] T. Franquet, K.S. Lee, N. Müller, Thin-section CT findings in 32 immunocompromised patients with cytomegalovirus pneumonia who do not have AIDS, AJR 181 (October (4)) (2003) 1059–1063, https://doi.org/10.2214/ajr.181.4.1811059.

[104] N.M. Vogel, H. Brodoefel, T. Hierl, et al., Differences and similarities of cytomegalovirus and pneumocystis pneumonia in HIV-negative immunocompromised patients: thin section CT morphology in the early phase of the disease, Br. J. Radiol. 80 (July (955)) (2007) 516–523, https://doi.org/10.1259/bjr/39696316.

[105] V.E. Chizhikov, C.F. Spiropoulou, S.P. Morzunov, et al., Complete genetic characterization and analysis of isolation of Sin Nombre virus, J. Virol. 69 (December (12)) (1995) 8132–8136, https://doi.org/10.1128/jvi.69.12.8132-8136.1995.

[106] G.W. Hallin, S.Q. Simpson, R.E. Crowell, et al., Cardiopulmonary manifestations of hantavirus pulmonary syndrome, Crit. Care Med. 24 (February (2)) (1996) 252–258, https://doi.org/10.1097/00003246-199602000-00012.

[107] L.H. Ketai, M.R. Williamson, R.J. Telepak, et al., Hantavirus pulmonary syndrome: radiographic findings in 16 patients, Radiology 191 (June (3)) (1994) 665–668, https://doi.org/10.1148/radiology.191.3.8184043.

[108] E.L. Gasparetto, T. Davaus, D.L. Escuissato, E. Marchiori, Hantavirus pulmonary syndrome: high-resolution CT findings in one patient, Br. J. Radiol. 80 (January (949)) (2007) e21–e23, https://doi.org/10.1259/bjr/30339154.